
**PLASMA, HYDRO-
AND GAS DYNAMICS**

Evolution of One-Dimensional Wind-Driven Sea Spectra¹

A. I. Dyachenko^{a, b, *}, D. I. Kachulin^a, and V. E. Zakharov^{a–d}

^a Novosibirsk State University, Novosibirsk, 630090 Russia

^b Landau Institute for Theoretical Physics, Russian Academy of Sciences, Chernogolovka, Moscow region, 142432 Russia

^c Department of Mathematics, University of Arizona, 857201 Tucson, AZ, USA

^d Lebedev Physical Institute, Russian Academy of Sciences, Moscow, 119991 Russia

* e-mail: alexd@itp.ac.ru

Received September 3, 2015

We analyze modern operational models of wind wave prediction on the subject for compliance dissipation. Our ab initio numerical simulations demonstrate that heuristic formulas for damping rate of free wind sea due to “white capping” (or wave breaking) dramatically exaggerates the role of this effect in these models.

DOI: 10.1134/S0021364015200035

1. INTRODUCTION

We perform numerical simulation of evolution of surface waves spectra that has been excited by wind. One of the motivation of writing this article is purely practical. Measure of nonlinearity of wave at the surface of deep water is their average steepness $\mu = \langle \nabla \eta^2 \rangle$, where $\eta(\mathbf{r}, t)$ is the shape of the surface. Characteristic value of μ in real sea is moderate, $\mu \simeq 0.06–0.07$. However, even at small steepness “white capping” (or wave breaking) happens occasionally, due to what waves loose energy. This phenomenon is not studied yet, either experimentally nor theoretically. Nevertheless, in the operational models of wind waves prediction heuristics formulas for rate of wave decay (due to this phenomenon) are widely used. They were introduced about thirty years before [1, 2] and little has changed since then. In our opinion, they have no serious justification. The goal of this article is to check these heuristic formulas by numerical experiments not assuming statistical description.

To study the white capping model with one horizontal dimension is enough. If steepness is moderate, $\mu \leq 0.07$, one can use the dynamical “Zakharov equation” [3], which is greatly simplified in 1-D case. It reduces to the simple Hamiltonian system that is very convenient for numerical simulation [4, 5]. Canonical transformation resulting in this model is described in detail in [6]. In the framework of this model, we perform numerical simulations for very long time (hundreds of thousands of characteristic wave period) and make sure that heuristic formulas [1, 2] give to large rates of energy decay. It makes to treat used below wave prediction operational models highly critical.

Another motivation for this work is the desire to describe (possible more in detail) a phenomenon of white capping for the waves with so moderate steepness. This work is not finished yet, but we established the most important fact: wave breaking is preceded by “freak wave” which actually breaks. Freak waves appear naturally as a result of modulational instability [3], but even stable spectra of moderate amplitude are able to generate them. Although freak waves are now rare events separated by time interval it tens of thousands of wave periods.

Finally, in this article we come back to the old question about integrability of the free surface hydrodynamics of the deep water. Hypothesis of integrability was formulated in [7] the result which was a key when deriving the compact equation [4, 5]. More recently, it was argued both against integrability [8, 9] and in favor integrability [10, 11]. In our experiments, we observed behavior that is typical for integrable systems. Dynamics of the wave field was quasi-periodical. Spectra averaged over great time (of the order of hundred thousand wave periods) have changed little, losing 15% of their energy due to arising rare freak waves.

As an initial condition we used experimental and often cited in the oceanographic literature JONSWAP spectrum [12] with the wind speed 12 m/s.

2. JONSWAP SPECTRUM

Hasselmann et al. [12] analyzed data collected during the Joint North Sea Wave Observation Project, and found that the wave spectrum is never fully developed. It continues to develop through nonlinear, wave–wave interactions even for very long times and

¹ The article is published in the original.

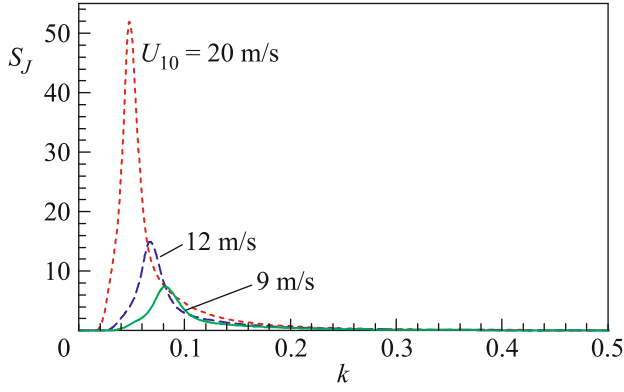


Fig. 1. (Color online) Energy density for the JONSWAP spectrum for different wind speeds.

distances. They therefore proposed a spectrum in the form:

$$S_J(\omega)d\omega = \alpha \frac{g^2}{\omega^5} \exp\left[-\frac{5}{4}\left(\frac{\omega_0}{\omega}\right)^4\right] \gamma^r d\omega, \quad (1)$$

$$r = \exp\left[-\frac{(\omega - \omega_p)^2}{2\sigma^2\omega_p^2}\right],$$

$$\alpha = 0.076 \left(\frac{U_{10}^2}{Fg}\right)^{0.22},$$

$$\omega_p = 22 \left(\frac{g^2}{U_{10}F}\right)^{1/3},$$

$$\sigma = \begin{cases} 0.07 & \text{if } \omega \leq \omega_p \\ 0.09 & \text{if } \omega > \omega_p. \end{cases}$$

Here, U_{10} is the wind speed at the altitude 10 m, F is fetch, i.e., distance from the shore. Spectra with different wind speeds are shown in Fig. 1.

In this work, we study the relaxation of this developed sea state.

3. COMPACT EQUATION FOR WATER WAVES

We start with the well-known Hamiltonian for water waves

$$H = \frac{1}{2} \int g\eta^2 + \psi \hat{k} \psi dx - \frac{1}{2} \int \{(\hat{k}\psi)^2 - (\psi_x)^2\} \eta dx + \frac{1}{2} \int \{\psi_{xx} \eta^2 \hat{k} \psi + \psi \hat{k} [\eta \hat{k} (\eta \hat{k} \psi)]\} dx + \dots, \quad (2)$$

which is expanded up to the fourth order as a function of Hamiltonian variables η and ψ (see [3]): after introducing complex canonical variables a_k

$$\eta_k = \sqrt{\frac{\omega_k}{2g}} (a_k + a_{-k}^*), \quad \psi_k = -i \sqrt{\frac{g}{2\omega_k}} (a_k - a_{-k}^*),$$

$$\omega_k = \sqrt{gk}$$

in [4, 5], we applied canonical transformation to the Hamiltonian variable a_k to introduce normal canonical variable $b(x, t)$:

- (i) $\eta_k, \psi_k \Rightarrow$ normal canonical variable a_k ,
- (ii) $a_k \Rightarrow b_k$.

This transformation explicitly uses vanishing of four-wave interaction and possibility to consider surface waves moving in the same direction, see [4, 5]. For this variable $b(x, t)$ Hamiltonian (2) acquires nice and elegant form:

$$\mathcal{H} = \int b^* \hat{\omega}_k b dx + \frac{1}{2} \int \left| \frac{\partial b}{\partial x} \right|^2 \left[\frac{i}{2} \left(b \frac{\partial b^*}{\partial x} - b^* \frac{\partial b}{\partial x} \right) - \hat{K} |b|^2 \right] dx. \quad (3)$$

The corresponding equation of motion is the following:

$$i \frac{\partial b}{\partial t} = \hat{\omega}_k b + \frac{i}{4} \hat{P} + \left[b^* \frac{\partial}{\partial x} (b'^2) - \frac{\partial}{\partial x} \left(b^* \frac{\partial}{\partial x} b^2 \right) \right] - \frac{1}{2} \hat{P}^+ \left[b \hat{k} (|b|^2) - \frac{\partial}{\partial x} [b' \hat{k} (|b|^2)] \right]. \quad (4)$$

The eigenvalue of the projection operator \hat{P}^+ in the Fourier space is the Heaviside step function:

$$P_k^+ = \theta(k) = \begin{cases} 1, & k > 0 \\ 0, & k \leq 0. \end{cases} \quad (5)$$

Transformation from $b(x, t)$ to physical variables $\eta(x, t)$ and $\psi(x, t)$ can be recovered from canonical transformation. It was derived in [6]. Here, we write this transformation up to the second order:

$$\eta(x) = \frac{1}{\sqrt{2}g^4} \left[\hat{k}^{\frac{1}{4}} b(x) + \hat{k}^{\frac{1}{4}} b(x)^* \right] + \frac{\hat{k}}{4\sqrt{g}} \left[\hat{k}^{\frac{1}{4}} b(x) - \hat{k}^{\frac{1}{4}} b(x)^* \right]^2,$$

$$\psi(x) = -i \frac{g^{\frac{1}{4}}}{\sqrt{2}} \left[\hat{k}^{-\frac{1}{4}} b(x) - \hat{k}^{-\frac{1}{4}} b(x)^* \right] + \frac{i}{2} \left[\hat{k}^{\frac{1}{4}} b^*(x) \hat{k}^{\frac{3}{4}} b^*(x) - \hat{k}^{\frac{1}{4}} b(x) \hat{k}^{\frac{3}{4}} b(x) \right] + \frac{1}{2} \hat{H} \left[\hat{k}^{\frac{1}{4}} b(x) \hat{k}^{\frac{3}{4}} b^*(x) + \hat{k}^{\frac{1}{4}} b^*(x) \hat{k}^{\frac{3}{4}} b(x) \right]. \quad (6)$$

Here, \hat{H} is the Hilbert transformation with the eigenvalue $i \text{sgn}(k)$.

4. KINETIC EQUATION

Along with simulation in the framework of Eq. (4), we solved the same initial problem with simple quasi-linear model

$$\frac{\partial |b_k|^2}{\partial t} = -\gamma_{\text{diss}} |b_k|^2, \quad (7)$$

performing averaging by time and wavenumbers, so that

$$|b_k|^2 \rightarrow n_k = \langle |b_k|^2 \rangle. \quad (8)$$

The constants γ_{diss} in Eq. (7) are:

$$\begin{aligned} \gamma_1^{\text{WAM3}} &= 3.33 \times 10^{-5} \bar{\omega} \left(\frac{\omega}{\bar{\omega}} \right)^2 \left(\frac{\bar{\alpha}}{\bar{\alpha}_{\text{PM}}} \right)^2, \\ \gamma_2^{\text{WAM3}} &= 2.33 \times 10^{-5} \hat{\omega} \left(\frac{\omega}{\hat{\omega}} \right)^2 \left(\frac{\hat{\alpha}}{\hat{\alpha}_{\text{PM}}} \right)^2. \end{aligned} \quad (9)$$

Here, $\bar{\omega}$ and $\hat{\omega}$ mean averaging over spectrum, α is an integral wave steepness, and

$$\bar{\alpha}_{\text{PM}} = E \bar{\omega}^4 g^{-2},$$

$$\bar{\alpha}_{\text{PM}} = 4.57 \times 10^{-3}$$

is the theoretical value of $\bar{\alpha}$ for a Pierson–Moskowitz spectrum [13], and

$$\hat{\alpha}_{\text{PM}} = 0.66 \bar{\alpha}_{\text{PM}};$$

E is the total energy (surface elevation variance). All these definitions are taken from operational models from [1, 2]. More recent models have just slight corrections to them. In this case model (7) is equivalent to the well-known Hasselmann kinetic equation [14] (see also [8]) because wind pumping is absent and collision term S_{nl} (due to the result of [7]) identically equal to zero. In both models, we add artificial damping

$$\Gamma_d(k) = \begin{cases} \alpha k^4 & \text{if the highest harmonics of } b_k \\ & \text{are } 10^4 \text{ times greater than} \\ & \text{the roundoff errors,} \\ 0 & \text{other wise} \end{cases} \quad (10)$$

with $\alpha = 0.9/\tau k_{\text{max}}^4$. It provides dissipation of extreme waves due to wave breaking. We calculated effective damping due to wave breaking, $\langle \gamma_{\text{diss}} \rangle$, plugging results of calculations in the framework of (4) into the Eq. (7). Another words we define $\langle \gamma_{\text{diss}} \rangle$ as following:

$$\gamma_{\text{diss}} = -\frac{1}{|b_k|^2} \frac{\partial |b_k|^2}{\partial t}. \quad (11)$$

5. EVOLUTION OF THE JONSWAP SPECTRUM

We study relaxation of developed sea with different wind speeds $U_{10} = 9, 12, \text{ and } 20$ m/s. However, in this

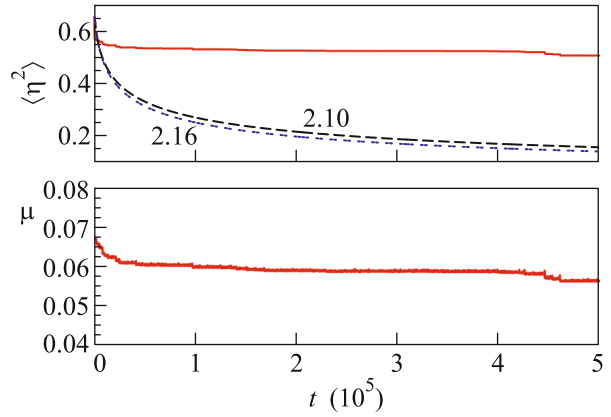


Fig. 2. (Color online) Energy density and steepness for the wind 12 m/s.

article we show results of simulation for $U_{10} = 12$ m/s only. The others are very similar. Periodic domain of the length $L = 10000$ m was used for numerical simulations. Initial conditions for b_k were chosen according to JONSWAP spectrum:

$$|b_k|^2 = \sqrt{\frac{2g}{\omega_k}} |\eta_k|^2 = S_J(k) \frac{2\pi g}{L \omega_k}. \quad (12)$$

Phases of b_k were chosen randomly in the interval $[0; 2\pi]$. Fetch F was equal to 157000 m.

We observed much smaller dissipation than predicts WAM3 model. For the wind velocity $U_{10} = 12$ m/s energy density both in our numeric experiment and calculated according to [1, 2] are shown in Fig. 2. Energy density is measured in oceanographic units

$$\frac{\text{energy density}}{g} = \text{m}^2.$$

The average steepness μ is calculated as following:

$$\mu = \sqrt{\int_{-\infty}^{\infty} k^2 |\eta_k|^2 dk}.$$

In the picture, one can see initial fast relaxation of energy in numerical experiment. It is due to dissipation of long tail $\simeq \omega^{-5}$ of JONSWAP spectrum in k -space (see (1)). After initial relaxation, there are rare events of energy dissipation in our experiment. Average steepness is also shown in the Fig. 2.

One of these rare events, wave breaking, taking place at time $\simeq 93340$, is shown in detail in the Fig. 3. One can see oscillation of the amplitude of the extreme wave.

The spectrum $S(k)$ along with the zoomed profile of the surface at time $\simeq 93340$ is shown in the Fig. 4. It is seen that the amplitude of the extreme (freak) wave is larger than for nearby waves by a factor of more than 3. Figure 4 also shows the energy spectrum $S(k)$

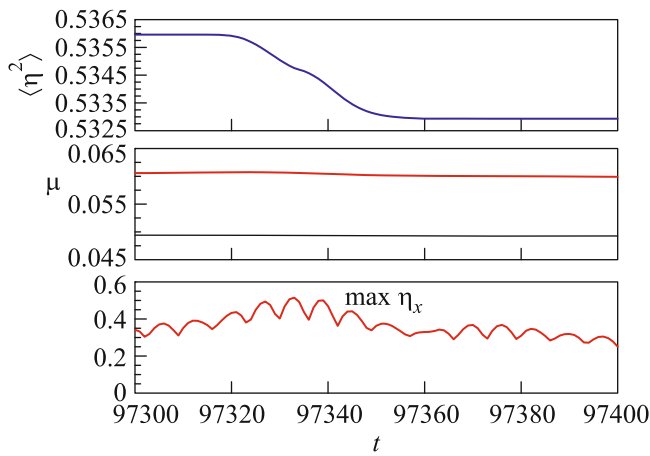


Fig. 3. (Color online) Drop of energy due to extreme wave appearing (wave breaking). Last picture shows maximal steepness of the extreme wave.

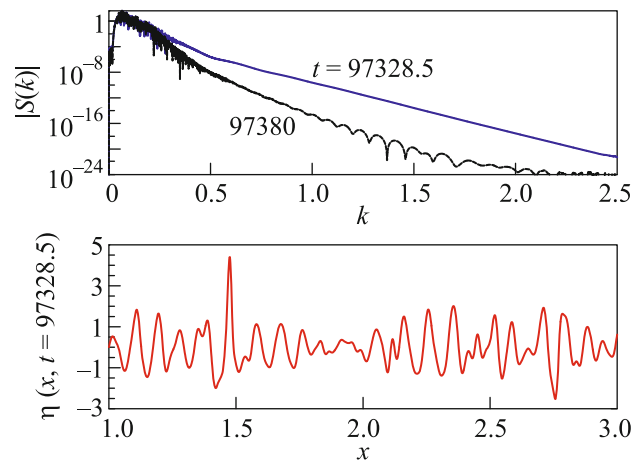


Fig. 4. (Color online) Spectral density $S(k)$ at the moment of freak wave appearing and freak wave almost 5 m height.

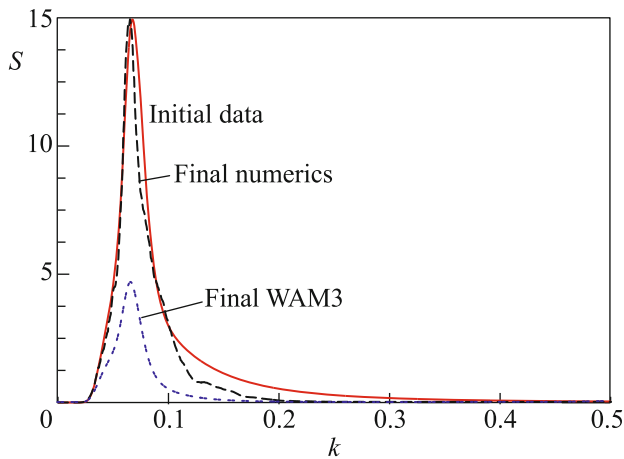


Fig. 5. (Color online) Spectral density $S(k)$ at initial moment (solid line), final numerical spectrum (dashed line), and final WAM3 spectrum (double dotted line).

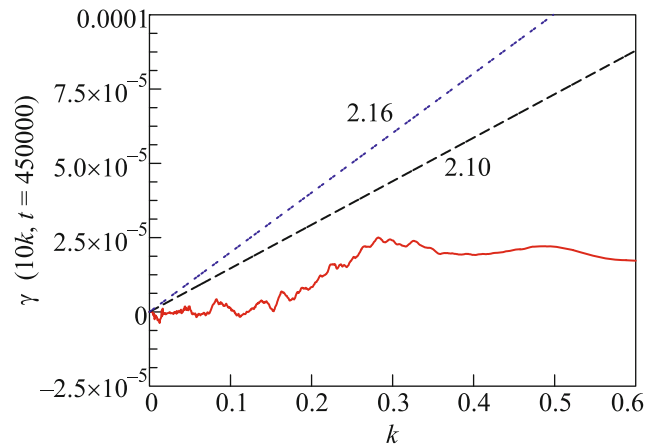


Fig. 6. (Color online) Comparison of γ_1^{WAM3} , γ_2^{WAM3} , and $\langle \gamma_{diss} \rangle$.

after wave breaking. It does not have tail at high wavenumbers.

Great difference between numerical results and prediction of the WAM3 model is seen in Fig. 5. Both of them had the same initial condition. However, at the final time the spectra are very different. The WAM3 model predicts much more energy dissipation. It is also seen in Fig. 2.

One can see that relaxation of energy is sufficiently long process. During hundreds of thousands seconds it decreases by $\approx 20\%$. During this time, we calculated average $\langle \gamma_{diss} \rangle$ according to (11). To make it smooth enough time of averaging was few hours (10000 s). According to [2] (Eqs. (2.10) and (2.16)) with (9) plotted by dotted and double dotted lines. $\langle \gamma_{diss} \rangle$ calculated with the use of dynamical equation with (10) shown

solid line. One can see that numerical experiment gives much less value of dissipation. Moreover, dissipation is absent in the core of spectral density where $k_0 \approx (0.06-0.07) \text{ m}^{-1}$.

6. CONCLUSIONS

The main result of our work is the fact that heuristic formulas for damping rate of free wind sea (9) due to white capping dramatically exaggerates the role of this effect. Especially convincing is Fig. 6 showing that in the region of spectral maximum dissipation of energy is practically absent. An increase in $\langle \gamma_{diss} \rangle$ with the wavenumber indicates that damping is concentrated in the region of high wavenumbers. It means that white capping leads primarily to vanishing of the spectra “tails” and smoothing of the wave field. We stress that our simulations describe sea evolution

during few days after “switch off” wind. During this time, sea lost no more than 20% of the energy. A similar picture of slow energy dissipation was observed in [15]. Because “dissipation function” γ_{diss} plays a key role in the massively used operational models, the inevitable conclusion is that these models need to be fundamentally reviewed.

Our simulations are another argument in favor of integrability of deep-water hydrodynamics. Others arguments in this favor are given in [10] and are very serious. There it is shown that exact system of Euler equations describing potential flow of deep water with a free surface can have any number of commuted integrals of motion. Weak point of this argument is the question about completeness of this system of integrals. In [9], it is shown that model (4) is not integrable. However, nonintegrability arises in the fifth order of perturbation theory where Eq. (4) strictly speaking is not applicable. The most serious arguments contained in [8], where indicated the non-existence of higher integrals.

This work was supported by the Russian Science Foundation (project no. 14-22-00174). The numerical simulation was performed at the Informational Computational Center, Novosibirsk State University.

REFERENCES

1. G. J. Komen, S. Hasselmann, and K. Hasselmann, *J. Phys. Oceanogr.* **14**, 1271 (1984).
2. The WAMDI Group, *J. Phys. Oceanogr.* **18**, 1775 (1988).
3. V. E. Zakharov, *J. Appl. Mech. Tech. Phys.* **9**, 190 (1968).
4. A. I. Dyachenko and V. E. Zakharov, *JETP Lett.* **93**, 701 (2011).
5. A. I. Dyachenko and V. E. Zakharov, *Eur. J. Mech. B: Fluids* **32**, 17 (2012).
6. A. I. Dyachenko, D. I. Kachulin, and V. E. Zakharov, in *Extreme Ocean Waves*, 2nd ed., Ed. by E. Pelinovsky and C. Harif (Springer, Berlin, 2016).
7. A. I. Dyachenko and V. E. Zakharov, *Phys. Lett. A* **190**, 144 (1994).
8. A. I. Dyachenko, Y. V. Lvov, and V. E. Zakharov, *Physica D* **87**, 233 (1995).
9. A. I. Dyachenko, D. I. Kachulin, and V. E. Zakharov, *JETP Lett.* **98**, 43 (2013).
10. V. E. Zakharov and A. I. Dyachenko, arXiv: 1206.2046.
11. A. I. Dyachenko and V. E. Zakharov, *JETP Lett.* **88**, 307 (2008).
12. K. Hasselmann, T. P. Barnett, E. Bouws, H. Carlson, D. E. Cartwright, K. Enke, J. A. Ewing, H. Gienapp, D. E. Hasselmann, P. Kruseman, A. Meerburg, P. Mller, D. J. Olbers, K. Richter, W. Sell, and H. Walden, *Ergaenzungsh. Deutsch. Hydrograph. Zeitschr.* **12**, 95 (1973).
13. W. Pierson and L. Moskowitz, *J. Geophys. Res.* **69**, 5181 (1964).
14. K. Hasselmann, *J. Fluid Mech.* **12**, 481 (1962).
15. V. E. Zakharov, A. O. Korotkevich, and A. O. Prokofiev, *AIP Conf. Proc.* **1168**, 1229 (2009).